ELSEVIER

Physica C 339 (2000) 245–252

PHYSICA C

www.elsevier.nl/locate/physc

Thermoelectric power and resistivity of $Nd_{1-x}Ca_xBa_2Cu_3O_y$ and $Nd_{1-x}La_xBa_2Cu_3O_y$

S.R. Ghorbani [a], M. Andersson [a,*], P. Lundqvist [a], M. Valldor [b], Ö. Rapp [a]

[a] *Solid State Physics, Royal Institute of Technology, SE-100 44 Stockholm, Sweden*
[b] *Inorganic Chemistry, Arrhenius Laboratory, Stockholm University, S-106 91 Stockholm, Sweden*

Received 1 February 2000; received in revised form 13 April 2000; accepted 18 April 2000

Abstract

The structural and transport properties of $Nd_{1-x}Ca_xBa_2Cu_3O_y$ ($x = 0.0$, 0.03, 0.06, and 0.10) and $Nd_{1-x}La_xBa_2Cu_3O_y$ (x nominally 0.0, 0.05, 0.10, and 0.15) have been studied by X-ray powder diffraction, electrical resistivity, and thermoelectric power measurements. In both series, the a- and b-axis lattice parameters decrease with increasing doping while the c-axis lattice parameter increases. The transport properties suggest improved metallic behaviour with increasing Ca doping in contrast to La doping. An anomalous sharp peak in the thermoelectric power close to T_c was observed, which depended on the doping content. We analysed the thermoelectric power as a function of temperature with a two-band model with an additional linear T term. An excellent agreement between model and data was obtained. © 2000 Elsevier Science B.V. All rights reserved.

PACS: 74.72.-h; 74.72.Jt; 74.25.Fy; 74.62.Dh
Keywords: Thermoelectric power; $NdBa_2Cu_3$; Substitution

1. Introduction

The normal state transport properties of oxide superconductors are unusual and systematic studies of them are therefore important for understanding the mechanism of high temperature superconductivity. Experiments have revealed a close relationship between the electronic properties of the cuprate high-T_c superconductors and the hole carrier concentration within the CuO_2 planes [1].

Since the original work on $La_{2-x}Sr_xO_4$ [2] and several high temperature superconductors have been found to show a parabolic variation of T_c with hole concentration [3]. A maximum in T_c has in many cases been found at an optimal value of the hole concentration, p, per planar Cu atom.

The thermoelectric power, S, is highly sensitive to the details of the charge concentration. In polycrystalline samples, grain boundaries will have less effect on S than on the electrical conductivity because the temperature drop between grains will usually be insignificant while the voltage drop is not.

Here, we report the results of X-ray diffraction (XRD), electrical resistivity, and thermoelectric power measurements on Ca- and La-doped $NdBa_2Cu_3O_y$ (Nd-123). In general, XRD shows small differences in structure with doping. From

* Corresponding author. Tel.: +46-8-790-7887; fax: +46-8-790-6952.
E-mail address: magnus@ftf.kth.se (M. Andersson).

0921-4534/00/$ - see front matter © 2000 Elsevier Science B.V. All rights reserved.
PII: S0921-4534(00)00346-4

the room temperature S, the hole concentration was estimated. The hole concentration changed with doping, which was consistent with the change in resistivity. From the relation between the hole concentration and doping concentration, it was inferred that some La atoms entered the Ba sites. The thermoelectric power was analysed and well described by a two-band model with an additional linear T term. The results also indicate an anomalous peak in S close to the transition temperature.

2. Experimental details

Samples of $Nd_{1-x}Ca_xBa_2Cu_3O_y$ (with $x = 0$, 0.03, 0.06, and 0.10) and $Nd_{1-x}La_xBa_2Cu_3O_y$ (with $x = 0$, 0.05, 0.10, and 0.15) were prepared by standard solid-state methods. Starting materials were of a high purity Nd_2O_3, $BaCO_3$, CuO, $CaCO_3$, and La_2O_3. The samples were pressed into pellets and calcinated at 900°C, 920°C, and 920°C with intermediate grindings. They were then annealed in flowing oxygen at 460°C for 3 days and the temperature was finally decreased to room temperature at a rate of 12°C/h.

The X-ray powder diffraction patterns were recorded in a Guinier–Hägg focusing camera using CuK_α radiation with Si as an internal standard [4]. The electrical resistivity was measured with a standard dc four-probe method. Electrical leads were attached to the sample by silver paint and heat treated at 300°C in flowing oxygen for half an hour, which gave contact resistances of order 1–2 Ω. T_c was taken as the mid point of the resistive transition. Thermoelectric power measurements were made on sintered bars of typical dimensions $0.5 \times 2.5 \times 10$ mm^3, using a small, reversible temperature difference of 1.5 K. The data were corrected for the contribution of the copper connecting leads. The sample holder with the possibility to measure two samples at the same time has been described elsewhere [5].

3. Results

3.1. X-ray diffraction

The samples were characterized by XRD. The Ca-doped samples displayed single-phase behaviour at these low doping levels with no additional lines. In the case of La doping, a few additional weak lines of $BaCuO_{2+v}$ were observed, which increased in intensity with an increasing La content. All XRD reflections in the Ca-doped series were indexed with an orthorhombic unit cell, and with the exception of at most six $BaCuO_{2+v}$ reflections, this was also the case for the La-doped samples. The effects of Ca and La substitution on the lattice constants are shown in Fig. 1. Substitution of Ca for Nd on the Nd sites results in a decrease in both

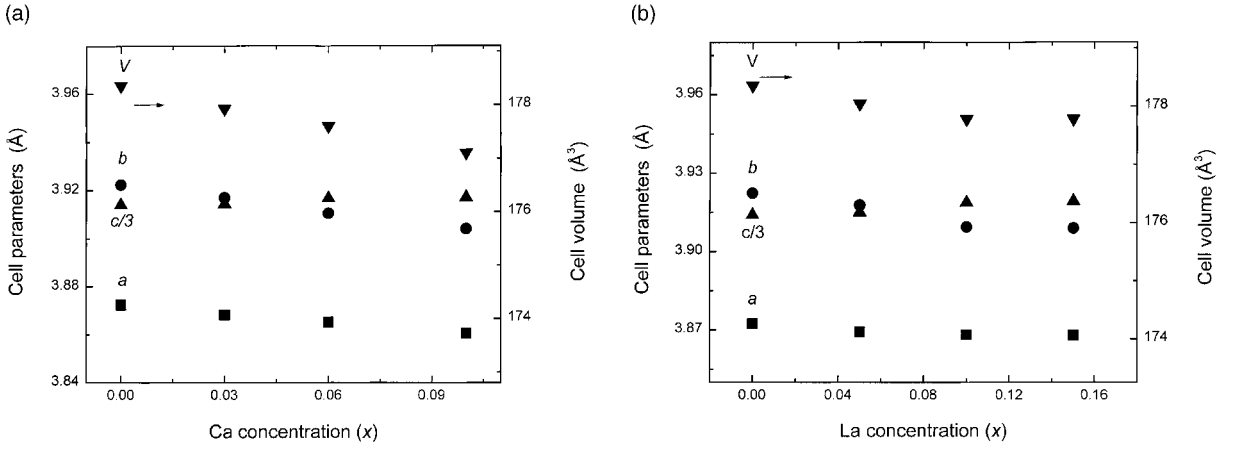

Fig. 1. Cell parameters of (a) $Nd_{1-x}Ca_xBa_2Cu_3O_y$ and (b) $Nd_{1-x}La_xBa_2Cu_3O_y$.

the *a*-, and *b*-axis lattice parameters and a small increase in the *c*-axis lattice parameter (Fig. 1(a)). The small changes are not surprising since the radius of Ca^{2+} is only slightly larger than that of Nd^{3+}. The faster decrease of the *b*-axis lattice parameter compared to the *a*-axis lattice parameter lead to a decrease in the orthorhombicity. This may suggest an increase in the oxygen occupancy along the *a*-direction (O(5) sites) [6], and/or an increase in oxygen vacancy concentration, in both cases pointing to an increased disorder in the CuO chains with increasing Ca content. La doping for Nd on the Nd sites also results in small decreases in the *a*- and *b*-axis lattice parameters, and a decrease of the orthorhombicity (Fig. 1(b)).

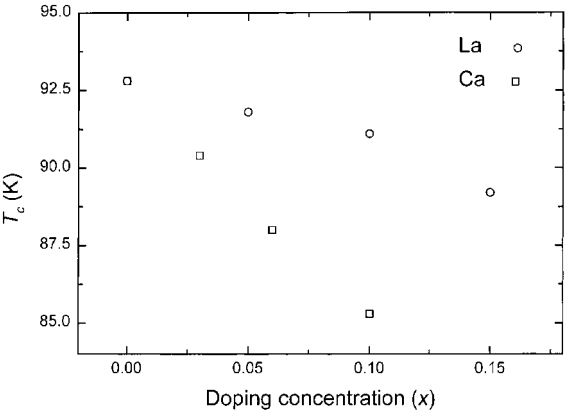

Fig. 3. Superconducting transition temperature versus doping concentration (*x*).

3.2. Electrical resistivity

The electrical resistivities of $Nd_{1-x}Ca_xBa_2Cu_3O_y$, and $Nd_{1-x}La_xBa_2Cu_3O_y$ are shown in Fig. 2. A linear resistivity in the normal state was observed for all samples. For $Nd_{1-x}Ca_xBa_2Cu_3O_y$ (Fig. 2(a)), the superconducting transition widths, ΔT_c, were quite narrow with widths (from 90% to 10% of the resistance drop), of 2.7, 2.0, 1.4, and 1.0 K for $x = 0$, 0.03, 0.06, and 0.10, respectively. For $Nd_{1-x}La_xBa_2Cu_3O_y$ (Fig. 2(b)), the superconducting transition widths, ΔT_c, were of 2.7, 4.6, 5.5, and 5.7 K for $x = 0$, 0.05, 0.10, and 0.15, respectively. The critical temperatures, T_c, is shown in Fig. 3 for Ca and La doping in Nd-123. The observed depression with increasing Ca content is consistent with that of $Y_{1-x}Ca_xBa_2Cu_3O_y$ [7], and can be explained by an increase in the total hole concentration in the planes because partial substitution with Ca^{2+} for Nd^{3+} introduces additional hole carrier in the structure and makes the $Nd_{1-x}Ca_xBa_2Cu_3O_y$ system accessible far into the overdoped region. The depression of T_c with La doping will be discussed below.

3.3. Thermoelectric power

Figs. 4 and 5 show the temperature dependence of the thermoelectric power for the $Nd_{1-x}Ca_xBa_2Cu_3O_y$, and $Nd_{1-x}La_xBa_2Cu_3O_y$ samples in the

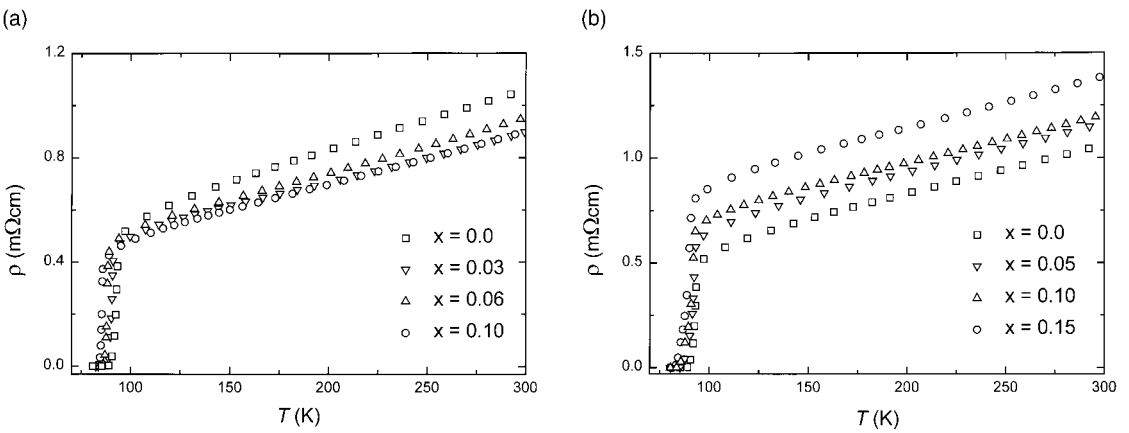

Fig. 2. The electrical resistivity versus temperature for (a) $Nd_{1-x}Ca_xBa_2Cu_3O_y$ and (b) $Nd_{1-x}La_xBa_2Cu_3O_y$.

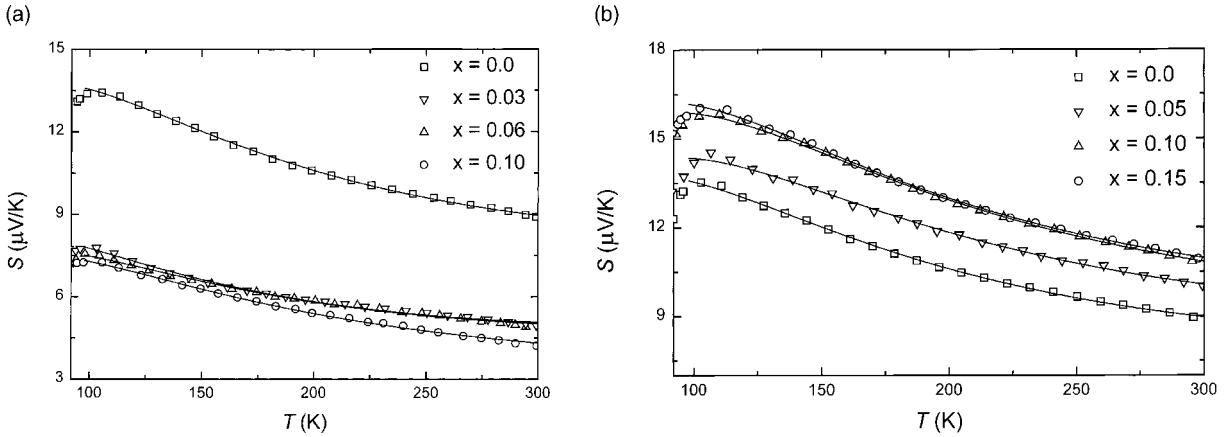

Fig. 4. The thermoelectric power versus temperature in the range 94–300 K. The solid curves fit to Eq. (1): (a) $Nd_{1-x}Ca_xBa_2Cu_3O_y$ and (b) $Nd_{1-x}La_xBa_2Cu_3O_y$.

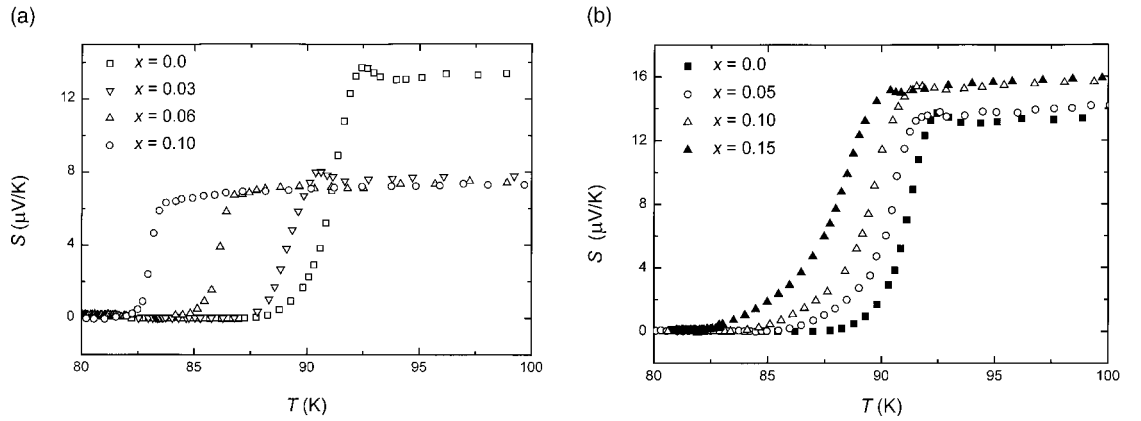

Fig. 5. The thermoelectric power versus temperature in the range 80–100 K. (a) $Nd_{1-x}Ca_xBa_2Cu_3O_y$ and (b) $Nd_{1-x}La_xBa_2Cu_3O_y$.

temperature range 94–300 K and 80–100 K, respectively. One can observe the following characteristics of the thermoelectric power with increasing Ca and La content: (i) The thermoelectric power is positive in the temperature range 80–300 K for all samples. (ii) Each S–T curve has a wide peak above the superconducting transition temperature. (iii) At high temperature, the thermoelectric power follows a linear temperature dependence with negative slope. (iv) In addition to the broad peak, an anomalous sharp peak is observed in the thermoelectric power close to T_c for some of the samples.

The thermoelectric power in the temperature range 100–300 K was analysed within a two-band model with an additional linear temperature term as suggested by Forro et al. [8], who used the following expression:

$$S = [AT/(B^2 + T^2)] + \alpha T,$$
$$A = 2(\varepsilon_0 - \varepsilon_F)/|e|, \quad (1)$$
$$B^2 = 3[(\varepsilon_0 - \varepsilon_F)^2 + \Gamma^2]/\pi^2 k_B^2.$$

The second term of S is the normal-band contribution. The first term, as proposed by Gottwick et al. [9] for analyses of the thermoelectric power

Table 1
The best-fit parameters A, B, and α of Eq. (1) and $(\varepsilon_0 - \varepsilon_F)$, Γ values determined from A and B

x	α (nV/K^2)	A (μV)	B (K)	$(\varepsilon_0 - \varepsilon_F)$ (K)	Γ (K)
$Nd_{1-x}Ca_xBa_2Cu_3O_y$					
0.0	8.5	2050	79	11.9	142
0.03	6.0	1020	65	5.9	118
0.06	5.6	1070	73	6.2	133
0.10	2.9	1100	76	6.4	137
$Nd_{1-x}La_xBa_2Cu_3O_y$					
0.05	9.0	2400	89	13.9	161
0.10	8.8	2670	88	15.5	160
0.15	9.8	2600	85	15.1	153

data of $CeNi_x$ samples, was obtained by assuming a superposition of a broad band and a localized band with a resonance peak in the density of state with width Γ at the position ε_0, close to the Fermi energy ε_F. The thermoelectric power of the $Nd_{1-x}Ca_xBa_2Cu_3O_y$, and $Nd_{1-x}La_xBa_2Cu_3O_y$ samples were well fitted to Eq. (1) as shown by the solid curves in Fig. 4. The points near T_c were not considered in these fits due to the sharp peak near T_c and the effect of superconducting fluctuation [10]. The results for the fitting parameters A, B, and α, are given in Table 1 along with the extracted values of $(\varepsilon_0 - \varepsilon_F)$ and Γ. To control the quality of the fitting, the profile factor (R) [1] was calculated. For $Nd_{1-x}Ca_xBa_2Cu_3O_y$, R-values were 5.2%, 6.6%, 7.6%, and 4.6% for $x = 0$, 0.03, 0.06, and 0.10, respectively, and for $Nd_{1-x}La_xBa_2Cu_3O_y$ they were 7.9%, 6.2%, and 6.3% for $x = 0$, 0.05, 0.10, and 0.15, respectively. The R-values are small indicating a good quality of the analyses. To estimate the sensitivity of the results for the parameters of Eq. (1), we changed each parameter until the R-value increased by a factor of 2, while the two other parameters were kept constant. For pure Nd-123, we then estimated the errors in the parameters to be of order 1%, 2%, and 5% for A, B, and α, respectively. The results for A and B illustrate that the analyses are quite sensitive to the difference $\varepsilon_0 - \varepsilon_F$.

[1] $R = \sum_i |y_{im} - y_{io}| / \sum_i y_{im}$, where y_{im} is the measured thermoelectric power and y_{io} is the corresponding thermoelectric power calculated from model.

4. Discussion

We start the discussion by considering the possibility of La doping on the Ba sites. Karen et al. [11] showed that partial substitution of Y with rear earths, REs, with large ion size resulted in samples containing a minor impurity of $BaCuO_{2+v}$. The tendency for substitution at the Ba sites increases with increasing size of the RE atom and is the most pronounced for La. If all of the La doping would enter the Nd sites in the $Nd_{1-x}La_xBa_2Cu_3O_y$ series, the hole concentration should be constant and the critical temperature would not change significantly. Substitution of La^{3+} for Ba^{2+} on the other hand results in a decrease in the hole concentration because the additional electrons contributed by La are expected to fill mobile holes. If all of the La doping would enter the Ba sites one would therefore expect the hole concentration to decrease linearly with increasing La doping with the same slope as when increasing the hole concentration with Ca doping.

In our case the XRD results indicate an increased amount of $BaCuO_{2+v}$ precipitates with increased La doping in qualitative agreement with Ref. [11]. Hole concentration was estimated from the relation between the room temperature $S_{290\,K}$ and hole concentration given by Obertelli et al. [12]. Fig. 6 suggests that increasing La doping cause a decrease in hole concentration smaller than for Ca doping, which shows that some La would enter the Ba sites. From the linear relation between hole concentration and doping concentration for La doping and comparing the slope with Ca doping as obtained by Bernhard et al. [13] and La

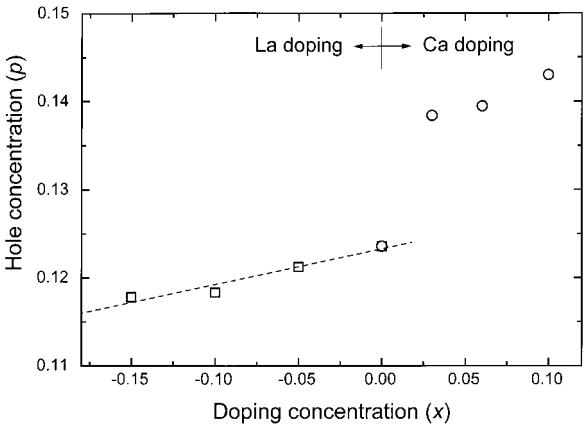

Fig. 6. Hole concentration versus doping concentration calculated from the model of Ref. [11]. The dashed line summaries data for La doping and was used to estimate Ba site occupancy as described in text.

doping in the Ba sites [14] in Y-123, [2] we inferred that 26% of the La atoms went to Ba sites, which is in good agreement with 29% as obtained for La doping in Y-123 by Karen et al. [11]. We note that our estimate may be affected by a changing oxygen content in the Ca-doped samples [15]. However, neutron powder diffraction studies on polycrystalline $Y_{1-x}Ca_xBa_2Cu_3O_y$ [7] and near-edge X-ray absorption spectroscopy on single crystal Y-123 [16] have not shown any change in the oxygen content for low doping concentration supporting our analysis.

For La doping, the increasing resistivity and the depression in the critical temperature are thus attributed to hole filling when substituting La for Ba. Increased La concentration resulted in an increase in the room temperature resistivity and a decrease in the temperature coefficient of resistance, and also in a decreasing hole concentration as shown in Fig. 7. These changes are all consistent with a decreasing hole concentration. For La doping, there is also an increase of the superconducting transition widths, ΔT_c.

Increased Ca doping resulted in a decrease in the room temperature resistivity and an increase in the temperature coefficient of resistance indicating improved metallic properties. This is in agreement with an increasing hole concentration as shown in Fig. 6. The superconducting transition widths, ΔT_c, decrease with increasing Ca content.

The wide peak in the thermoelectric power above the superconducting transition shifts towards higher temperatures for Ca doping and towards higher temperature for La doping. As an alternative to the model of Eq. (1), one can consider the presence of disorder in a periodic system where localisation of the electronic states in the tails of the conduction band occurs below a mobility edge ε_C separating localized and extended states [17]. It has been suggested [18] that the shift of the observed peak arises with carrier concentration since the temperature corresponding to the wide peak changes linearly with $\varepsilon_C - \varepsilon_F$. This difference increases or decreases with decreasing or increasing carrier concentration, which to some extent is supported by the results in Table 1 and by the resistivity. Since the chain contribution to S gives a large positive slope while the plane contribution typically gives rise to a negative slope [12,19], the results in Fig. 4 indicate that holes in CuO chains do not contribute to the thermoelectric power. The anomalous sharp peak close to T_c (Fig. 5) is attributed to fluctuation effects as calculated by Lu et al. [20]. The width of this anomalous peak increases with increasing La content and the peak has disappeared for $x = 0.06$ when doping with Ca (see Fig. 5(a)).

[2] We could not estimate the exact La concentration on the Ba sites from the slope of Nd-123 doped by Ca, because a few Nd atoms enter the Ba sites [11].

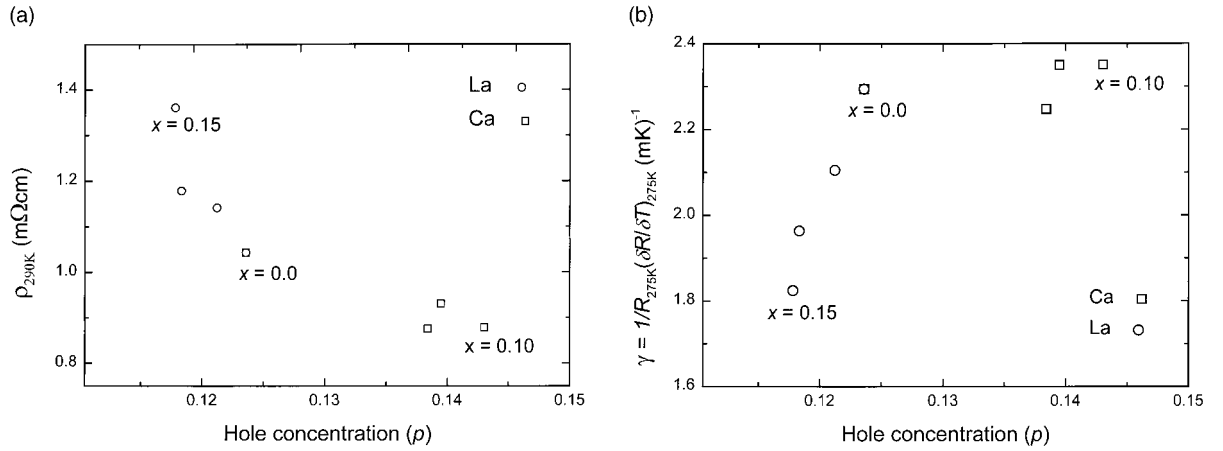

Fig. 7. (a) The room temperature resistivity versus hole concentration (p). (b) The temperature coefficient of resistivity at 275 K.

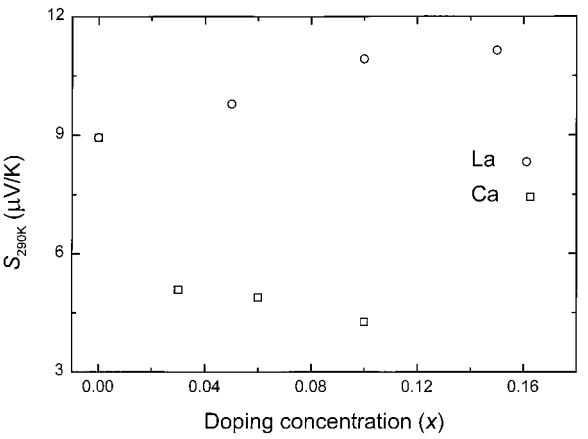

Fig. 8. The room temperature thermoelectric power versus doping concentration (x).

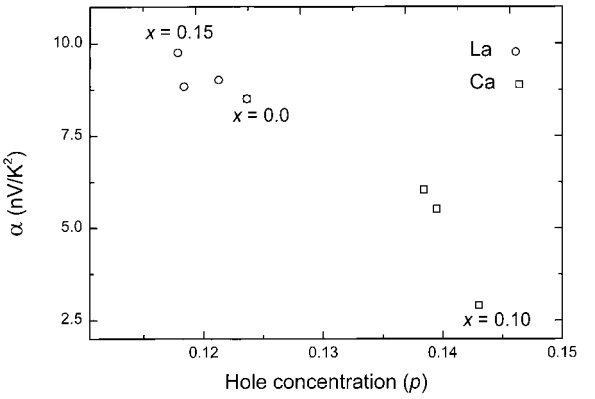

Fig. 9. α versus hole concentration (p).

The room temperature thermoelectric power ($S_{290\,K}$) is shown in Fig. 8. $S_{290\,K}$ decreases or increases with increasing Ca (La) doping, apparently associated with an increase or decrease in carrier concentration in the plane. $S_{290\,K}$ for Ca doping is small in agreement with the improved metallic properties suggested from the resistivity measurements.

In the analysis of Eq. (1), α is positive for all the samples (Fig. 9). With the increase of La doping, i.e., with a decrease of the carrier concentration, $(\varepsilon_0 - \varepsilon_F)$ increases similar to results for $Bi_2Sr_2Ca_{1-x}Y_xCu_2O_{8+\delta}$ [21] and $Tl_2Ba_2Ca_{1-x}Y_xCu_2O_{8+\delta}$ [22] samples. It is known that, with decreasing hole concentration, the Fermi energy should go up relative to the top of the band. Therefore, if ε_0 is fixed in position, these results suggest that ε_F must decrease with decreasing hole concentration, which is not expected. To resolve a similar problem Mandal et al. [21] assumed that the ε_0 position may shift upwards with decreasing hole concentration. However, no systematic variation of Γ with doping concentration was observed.

In summary, La and Ca doped Nd-123 were found to have a positive thermoelectric power, which increased with increasing La doping and decreased with Ca doping. The room temperature resistivity and thermoelectric power indicate that

hole concentration increased with increasing Ca doping and decreased with increasing La doping. We inferred from the results that 26% of the La atoms are substituted on the Ba sites. An anomalous sharp peak was observed in the thermoelectric power close to T_c and was dependent on doping content. The width of this anomalous peak increased with increasing La doping and the peak vanished for Ca doping above $x = 0.06$. A two-band model with an additional linear T term could well describe the results for the thermoelectric power.

Acknowledgements

We would like to thank Ingrid Bryntse, Stockholm University, for the help provided to prepare the samples. S.R.G acknowledges the financial support of the Ministry of Culture and Higher Education (MCHE) of I.R. Iran. Financial supports from the Swedish Natural Science Research Council (NFR) and the Swedish Superconductivity Consortium are gratefully acknowledged.

References

[1] B. Batlogg, H.Y. Hwang, H. Takagi, R.J. Cava, H.L. Kao, Physica C 235–240 (1994) 130.
[2] J.B. Torrance, Y. Tokura, A.I. Nazzal, A. Bezing, T.C. Huagan, S.S.P. Parkin, Phys. Rev. Lett. 61 (1988) 1127.
[3] M.R. Presland, J.L. Tallon, R.G. Buckley, R.S. Liu, N.E. Flower, Physica C 176 (1991) 95.
[4] K.E. Johansson, P.E. Werner, J. Phys. E 13 (1989) 1289.
[5] M. Rodmar, Ph.D. Thesis, Royal Institute of Technology, Stockholm, Sweden, 1999, TRITA-FYS 5246.
[6] P. Lundqvist, Ö. Rapp, R. Tellgren, I. Bryntse, Phys. Rev. B 56 (1997) 2824.
[7] G. Böttager, I. Mangelschots, E. Kaldis, P. Fischer, Ch. Kruger, F. Fauth, J. Phys. Cond. Matter 8 (1996) 8889.
[8] L. Forro, J. Lukatela, B. Keszei, Solid State Commun. 73 (1990) 501.
[9] U. Gottwick, K. Gloos, S. Horn, F. Steglich, N. Grewe, J. Magn. Mater. 47–48 (1985) 536.
[10] K. Maki, J. Low Tem. Phys. 14 (1974) 419.
[11] P. Karen, H. Fjellvåg, O. Braaten, A. Kjekshus, H. Bratsberg, Acta Chem. Scan. 44 (1990) 994.
[12] S.D. Obertelli, J.R. Cooper, J.L. Tallon, Phys. Rev. B 46 (1992) 14928.
[13] C. Bernhard, J.L. Tallon, Phys. Rev. B 54 (1996) 10201.
[14] V.E. Gasumyants, E.V. Vladimirskaya, Phys. Solid State 40 (1) (1998) 14.
[15] J.T. Kucera, J.C. Bravman, Phys. Rev. B 51 (1995) 8582.
[16] M. Merz, N. Nucker, P. Schweiss, S. Schuppler, C.T. Chen, V. Chakarian, J. Freeland, Y.U. Idzerda, M. Kläser, G. Muller-Vogt, Th. Wolf, Phys. Rev. Lett. 80 (1998) 5192.
[17] N.F. Mott, E.A. Davis, Electronic Processes in Non-Crystalline Materials, second ed., Oxford University Press, Oxford, UK, 1979.
[18] J.B. Mandal, A.N. Das, B. Ghosh, J. Phys. Cond. Matter 8 (1996) 3047.
[19] M. Staines, J.L. Tallon, R. Meinhold, Physica C 258 (1996) 273.
[20] Y. Lu, B.R. Patton, J. Phys. Cond. Matter 7 (1995) 9247.
[21] J.B. Mandal, S. Keshri, P. Mandal, A. Poddar, A.N. Das, B. Ghosh, Phys. Rev. B 46 (1992) 11840.
[22] S. Keshri, J.B. Mandal, P. Mandal, A. Poddar, A.N. Das, B. Ghosh, Phys. Rev. B 47 (1993) 9048.